



# In situ atomic force microscopy of partially demineralized human dentin collagen fibrils

Stefan Habelitz,<sup>a,\*</sup> Mehdi Balooch,<sup>b</sup> Sally J. Marshall,<sup>a</sup> Guive Balooch,<sup>a</sup>  
and Grayson W. Marshall, Jr.<sup>a</sup>

<sup>a</sup> Department of Preventive and Restorative Dental Sciences, University of California, 707 Parnassus Avenue D-2260, San Francisco, CA 94143, USA

<sup>b</sup> Department of Chemistry and Materials Science, Lawrence Livermore National Laboratory, Livermore, CA 94550, USA

Received 26 December 2001, and in revised form 29 May 2002

## Abstract

Dentin collagen fibrils were studied in situ by atomic force microscopy (AFM). New data on size distribution and the axial repeat distance of hydrated and dehydrated collagen type I fibrils are presented. Polished dentin disks from third molars were partially demineralized with citric acid, leaving proteins and the collagen matrix. At this stage collagen fibrils were not resolved by AFM, but after exposure to NaOCl<sub>aq</sub> for 100–240 s, and presumably due to the removal of noncollagenous proteins, individual collagen fibrils and the fibril network of dentin connected to the mineralized substrate were revealed. High-aspect-ratio silicon tips in tapping mode were used to image the soft fibril network. Hydrated fibrils showed three distinct groups of diameters: 100, 91, and 83 nm and a narrow distribution of the axial repeat distance at 67 nm. Dehydration resulted in a broad distribution of the fibril diameters between 75 and 105 nm and a division of the axial repeat distance into three groups at 67, 62, and 57 nm. Subfibrillar features (4 nm) were observed on hydrated and dehydrated fibrils. The gap depth between the thick and thin repeating segments of the fibrils varied from 3 to 7 nm. Phase mode revealed mineral particles on the transition from the gap to the overlap zone of the fibrils. This method appears to be a powerful tool for the analysis of fibrillar collagen structures in calcified tissues and may aid in understanding the differences in collagen affected by chemical treatments or by diseases. © 2002 Elsevier Science (USA). All rights reserved.

**Keywords:** Dentin; Collagen; Atomic force microscopy; Hydration

## 1. Introduction

Dentin is the calcified tissue that forms the internal bulk of the tooth, lying between the enamel and the pulp chamber. It is a hydrated biological composite consisting of tubules, which were the pathways of the formative odontoblastic cells, the peritubular dentin, a highly mineralized zone surrounding the tubules, and the intertubular dentin (Ten Cate, 1994). The latter has an estimated composition of approximately 50 wt% mineral phase, 40 wt% organic phase, and 10 wt% aqueous fluids and is similar to the composition of bone (Weiner and Wagner, 1998). Ninety weight percent of the organic phase in dentin is collagen, which is almost exclusively type I (Goldberg and Takagi, 1993; Linde and Robins,

1988). Type I collagen forms a fibrous three-dimensional network which builds up the dentin matrix. Compared to bone, the collagen matrix in dentin is more interwoven with numerous crossings of fibrils (Kramer, 1951). Noncollagenous proteins, mostly glycoproteins and proteoglycans, cover the collagen fibrils and are associated with the inorganic phase. In particular, phosphoproteins are believed to be critical for inducing mineral nucleation and for binding to calcium phosphates (Begue-Kirn et al., 1998; Dahl et al., 1998; MacDougall et al., 1992; Saito et al., 1998). The mineral in dentin is a carbonated apatite, which is similar to the mineral in bone and calcified tendon and is located either in the gaps between collagen molecules (intrafibrillar) or attached to the collagen fibrils (extrafibrillar) (Lees et al., 1997; Wassen et al., 2000). Plate-like and cylindrical morphologies have been reported for the apatite crystals in dentin with dimensions between 20 and 5 nm (Arsenault, 1989; Kinney et al., 2001; LeGeros, 1991).

\* Corresponding author. Fax: +415-476-0858.

E-mail address: shabeli@itsa.ucsf.edu (S. Habelitz).

The structure–property relationship of collagen fibrils is critical for understanding many aspects of this tissue: alteration with disease, aging, or restorative treatments such as dentin bonding. Type I collagen molecules are composed of three supercoiled polypeptide chains of about 290 nm in length, held together by water bridges and hydrophobic cross-links. During dentinogenesis, collagen molecules are synthesized at the rough endoplasmic reticulum of the odontoblasts and extruded as a triple helix (tropocollagen) into the extracellular space. In a current model, five tropocollagen molecules stagger longitudinally, overlapping by about one quarter of their length, to form a microfibril about 4 nm in diameter (Nimni and Harkness, 1988). The microfibrils aggregate with their long axes in parallel to form collagen fibrils. *In vitro* observations of the fibrillogenesis showed an increase of the fibril diameter by increments of approximately 8 nm, attributed to units of microfibrils, which are the building blocks of the collagen fibril (Parry and Craig, 1988; Prockop and Fertala, 1998). Depending on the tissue type, age, and genetic defects, collagen fibrils vary in diameter from 30 to 500 nm, as determined by electron microscopy and X-ray diffraction (XRD) (Nimni and Harkness, 1988). Shrinkage due to dehydration by 10–40% has been reported (Brodsky et al., 1988). Human dentin collagen fibrils have been imaged at high resolution by electron microscopy. However, the fibril diameters reported were not consistent among studies. Fibril diameters around 100 nm have frequently been determined (Garberoglio and Brännström, 1976; Pashley, 1991; Perdigão et al., 1996), but values as low as 30–60 nm were also found in the literature (Avery, 1988; Lin et al., 1993). Lin et al. (1993) reported fibrils of increased thickness at the dentino–enamel junction, with diameters between 80 and 120 nm.

The hierarchical synthesis of collagen fibrils leads to a high degree of organization and yields a strongly crystalline character, which is even more pronounced when the fibril is hydrated (Prockop and Fertala, 1998). The staggered arrangement, combined with gaps between the ends of successive collagen molecules, results in periodically alternating gaps and overlap zones. Their periodicity, or D-distance, depends on the state of hydration of the fibril and decreases from 67 nm for the hydrated fibril, to around 64 nm in air-dried samples, and down to 60 nm after dehydrothermal treatments at 120 °C (Baer et al., 1988; Bella et al., 1995; Wess and Orgel, 2000).

*In situ* observation of details of dentin collagen structure has largely been achieved by electron microscopy (Arsenault, 1989; Lin et al., 1993; Perdigão et al., 1999). Usually transmission electron microscopy (TEM) has been used to obtain the high resolution necessary to observe the structural features of the fibrils. TEM studies, however, require intensive sample preparation and often staining to resolve gap and overlap zones of

collagen fibrils. Furthermore, the vacuum in electron microscopy does not facilitate imaging of the tissue in its natural hydrated state and raises concerns of introducing artifacts due to desiccation (El Feninat et al., 2001; Lee, 1984; Reedy et al., 1983). TEM studies frequently showed an axial repeat distance around 64 nm, attributed to the dehydrated fibril. Beniash et al. (2000) avoided fibril contraction during TEM observation by using vitrified ice sections and determined a D-periodicity of 67 nm, as documented for the hydrated fibril. They also reported D-distances as low as 23.5 nm for forming fibrils in rat pre-dentin, with diameters of around 30 nm.

Scanning probe microscopes and, in particular, the atomic force microscope have facilitated the imaging and analysis of biological surfaces with little or no sample preparation. Atomic force microscopy (AFM) can operate in air or in liquid, and the imaging of macromolecules, like proteins or DNA, has been reported by several authors (Chen and Hansma, 2000; Hansma, 2001; Scheuring et al., 2001). Assembled proteins, e.g., collagen fibrils, also have been resolved successfully. Several authors (Chernoff and Chernoff, 1992; Raspanti et al., 1997; Revenko et al., 1994) revealed the D-periodicity of reconstituted collagen fibrils on a mica or glass substrate using AFM. Subfibrillar structures of 4–5 nm of dehydrated native rat tail and reconstituted bovine dermal collagen were resolved by Baselt et al. (1993). Reconstitution of collagen fibrils, however, involves a series of chemical treatments to first dissolve and then reassemble the fibrils. Thus, the fibril is no longer imaged in its native environment and original structural features could be lost or altered during reassembly.

The composite nature of dentin and bone, where fibrils are covered by noncollagenous matrix proteins and apatite minerals, increases the difficulty of imaging of the fibrils by topographic techniques like AFM. Recent *in situ* studies of sequential demineralization and deproteinization of dentin have shown that, under certain circumstances, high-resolution AFM imaging of collagen fibrils is possible (Marshall et al., 2001). This suggested that dissolution of most of the mineral phase, followed by gradual removal of extracellular matrix proteins, would expose collagen fibrils, which could be revealed by AFM. In the present study, this method is applied to dentin to obtain information on collagen fibril organization and the effects of hydration and dehydration on fibril diameter and axial repeat distance.

## 2. Materials and methods

Human third molars with documented history were extracted from patients of ages of between 22 and 34 years according to protocols approved by the University

of California, San Francisco Committee on Human Research. Teeth were sterilized by  $\gamma$ -radiation and stored in deionized water at 4°C until prepared (White et al., 1994). Sagittal midcoronal sections of six teeth (thickness of 2 mm) were prepared by polishing through a series of SiO<sub>2</sub> papers and with water-based diamond paste to 0.25  $\mu$ m (Buehler, Lake Bluff, IL). Ultrasonic treatments in water for 10 s were used to clean the surface. Specimens were etched with 10 vol% citric acid (C<sub>6</sub>H<sub>8</sub>O<sub>7</sub>) for 15 s. The application of acids such as citric acid dissolves the mineral in calcified tissues and leaves the organic phases behind. Dentin etching is a common technique for providing a better substrate for bonding to dental adhesives (Marshall et al., 1997). Subsequently, specimens were treated with an aqueous solution of 6.5 vol% sodium hypochlorite (NaOCl<sub>aq</sub>) at time intervals of 10–20 s for up to 300 s total time (Marshall et al., 2001). Sodium hypochlorite is used as a cleansing, disinfective, nonspecific deproteinizing agent in endodontic treatments. In aqueous solutions superoxide radicals (O<sub>2</sub><sup>-</sup>) are formed and induce one-electron oxidations that fragment long peptide chains of proteins. NaOCl<sub>aq</sub> also is believed to chlorinate protein terminal groups, forming *N*-chloroamines, which are then broken down (Di Renzo et al., 2001; Pereira et al., 1973).

AFM images in the midcoronal area of demineralized dentin were obtained at each NaOCl treatment interval. Once the collagen fibril network was observed in contact mode at large scan sizes (about 10  $\times$  10  $\mu$ m), particular areas of the specimen were studied at high resolution in tapping mode. AFM studies were performed on a Multi Mode Nanoscope III using a calibrated vertical-engage “JV” piezo-scanner (Digital Instruments, Santa Barbara, CA). Contact mode images were obtained in liquid with Si<sub>3</sub>N<sub>4</sub>-tips (NP), (Digital Instruments). For high-resolution images in air, high-aspect-ratio Si-tips (Nanosensor, Wetzlar, Germany) with a radius of approximately 10 nm were used at resonance frequencies near 330 kHz. Specimens were dehydrated by air-blowing (5 s) and continued drying in air for at least 1 h before imaging. Hydrated samples were imaged in Hanks balanced salts solution using Nanoprobe SPM tips (FIB Spike) at a resonance frequency around 165 kHz. Tapping and phase mode images were recorded simultaneously at scanning rates as low as 0.3 Hz for scan sizes below 1  $\times$  1  $\mu$ m. Phase mode imaging is sensitive to the elastic properties of the substrate. The phase lag, which is recorded during scanning in tapping mode, is used to create a phase image, which is based on both the topography and the elastic response of the substrate to the tapping tip (Burnham et al., 1997).

Collagen fibril diameter and axial repeat distance were measured from section analysis of images using data that had been modified only by plane fitting. Section analysis was used to determine the step height between the gap and overlap zones of individual fibrils.

The collagen fibril diameter was preferentially determined from fibrils that exposed their complete diameter, by measuring the radius of curvature across the overlap zone, assuming a circular transverse shape. A total of 395 and 180 diameters of individual fibrils were analyzed in the hydrated and dehydrated states, respectively. Measurements of fibril dimensions were corrected for the tip radius. The dimensions necessary to calculate the radius of the AFM silicon tips were determined from high-resolution SEM images (Hitachi, model S-4500 with cooled cathode field emission capability with nanometer resolution). A parabola of the form  $Y = aX^2 + bX + c$  was fitted to the profile using standard least-squares software. The tip radius ( $r$ ) at its apex is given by  $1/(2a)$  (typically a 5 to 10-nm radius of curvature). The fibril diameters obtained from the radius of curvature were corrected for tip broadening by the equation  $e = 2r$ , where  $e$  is the error in the horizontal dimension (Takeyasu et al., 1996).

Axial repeat distances of individual collagen fibrils were determined from AFM images by Fourier transform analysis (AFM software 4.48r, Digital Instruments) of spectral frequencies along a line placed parallel onto the fibril axes. A total of 322 and 363 periodicities of fibrils were measured in the hydrated and dehydrated states, respectively. The values obtained for the diameter and periodicity of each fibril were rounded to the full nanometer.

### 3. Results

Figs. 1a–d show a series of 10  $\times$  10- $\mu$ m contact mode images of hydrated human intertubular dentin after different chemical treatments. The polished and untreated tooth specimen of Fig. 1a shows its characteristic structure (Marshall et al., 1997). A layer of higher mineralization, the peritubular dentin, lines tubules of about 1  $\mu$ m in diameter. The matrix phase between the tubules is intertubular dentin, consisting of extracellular matrix proteins and carbonated apatite mineral. Fig. 1b shows the microstructure of human dentin after acid treatment with 10 vol% citric acid for 15 s (Marshall et al., 1993). Dentinal tubule diameters are increased due to the recession of the peritubular dentin. As shown in an earlier study, this treatment demineralized about 700 nm deep into the intertubular dentin (Marshall et al., 2001). The demineralized layer consists predominantly of collagen and other matrix proteins. In the next step, 6.5 vol% NaOCl<sub>aq</sub> (bleach) was applied to etched specimens, and their surfaces were imaged at time intervals of 10–20 s. A dense network of fibrils became visible after an accumulation of 70 s of treatment with 6.5% NaOCl<sub>aq</sub>. The image quality of the fibrillar network improved with bleaching time and appeared to be optimized for times between 100 and 200 s

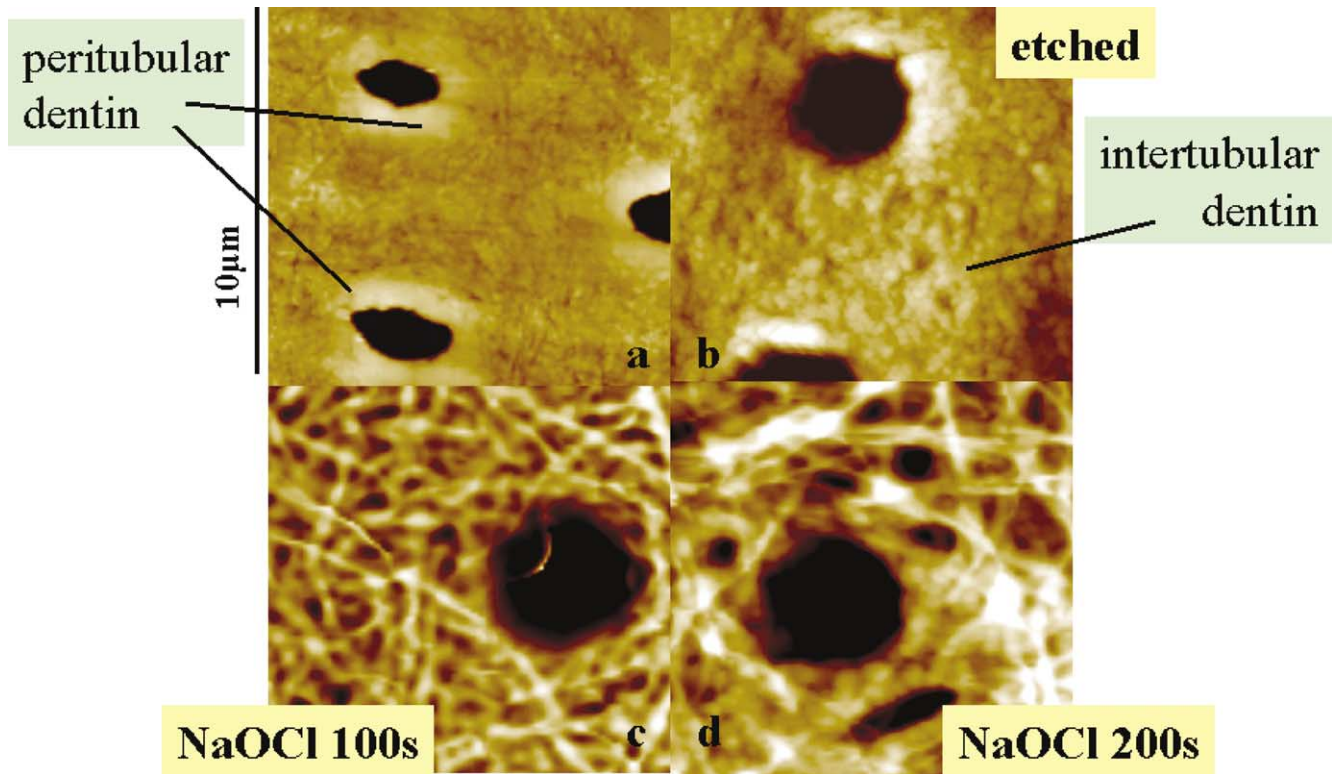


Fig. 1. Contact mode AFM images of the occlusal section of human dentin. (a) Untreated polished sample showing dentin tubules surrounded by peritubular dentin and the intertubular matrix; (b) after partial demineralization by 10 vol% citric acid for 15 s, peritubular dentin is dissolved; (c) subsequently treated with 6.5 vol% NaOCl<sub>aq</sub> for 100 s; and (d) subsequently treated with 6.5 vol% NaOCl<sub>aq</sub> for 200 s. Collagen fibrils are revealed. All images were obtained in liquid.

(Figs. 1c and d). The number of fibrils decreased with bleaching time. NaOCl<sub>aq</sub> treatments for more than 240 s led to the total removal of collagen fibrils, leaving behind a “moth-eaten” appearance of dentin caused by the demineralization and deproteinization of dentin that exposed dentinal tubules, microtubules, and numerous interconnections (Marshall et al., 2001).

Specimens, which were treated with NaOCl<sub>aq</sub> for times from 110 to 200 s and exhibited the fibrillar network of collagen in the contact mode using a Si<sub>3</sub>N<sub>4</sub>-tip, were then examined in air and buffered solutions using a high-aspect-ratio Si-tip in tapping mode. Fig. 2 shows an overview of the fibril organization and their random orientation at a scan size of 2.3 µm. At this magnification, the fibril periodic pattern appeared. Fig. 3a is a mixed-mode surface plot obtained in liquid exhibiting the fibrillar structure and the axial repeat pattern of collagen type I. Interlocking of gap and overlap regions of neighboring fibrils is observed. Fig. 3b is a surface plot of dentin collagen obtained in air after drying. The axial repeat pattern remains after dehydration. Fig. 4 contains topographic (a) and phase mode (b) images obtained in liquid on demineralized and bleached dentin of the same area. Both image modes exhibit the characteristic structure of collagen fibrils and are suitable for measuring the dimensions of fibril features. Phase mode

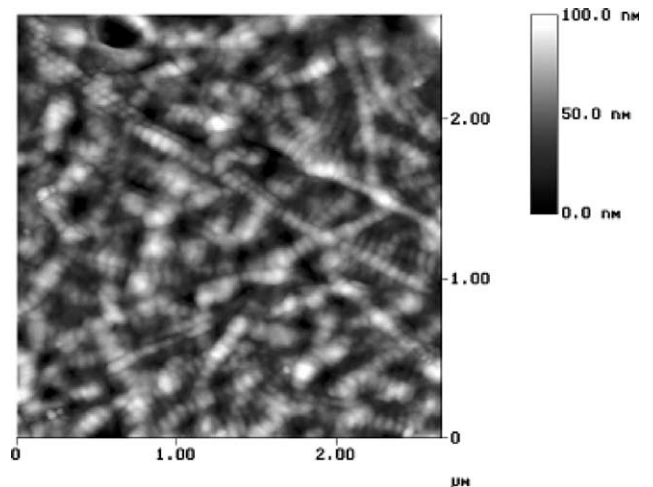


Fig. 2. Tapping mode AFM image of dentin collagen fibrils, obtained from demineralized specimen (15 s citric acid) treated with 6.5 vol% NaOCl<sub>aq</sub> for 130 s and in air, showing the repeat pattern and the random distribution of fibrils in intertubular dentin.

imaging, however, also is sensitive to the elastic properties of the substrate, and differences in the stiffness of the substrate can be revealed (Behrend et al., 1999). The phase mode image in Fig. 4b shows two darker spots on the transition from the gap to the overlap zone of the

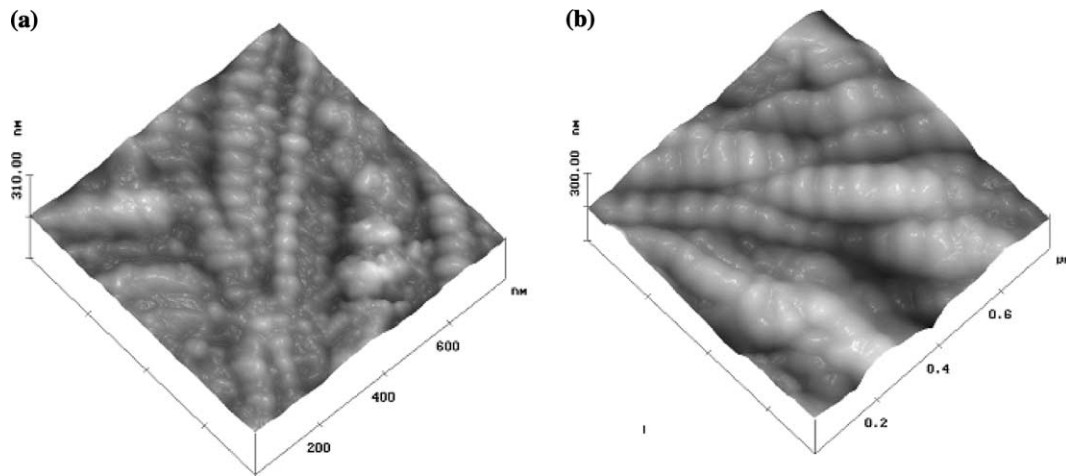


Fig. 3. Mixed-mode surface plots of tapping and phase mode AFM images of dentin collagen fibrils, obtained (a) in liquid and (b) in air. The axial repeat pattern is still present after dehydration.

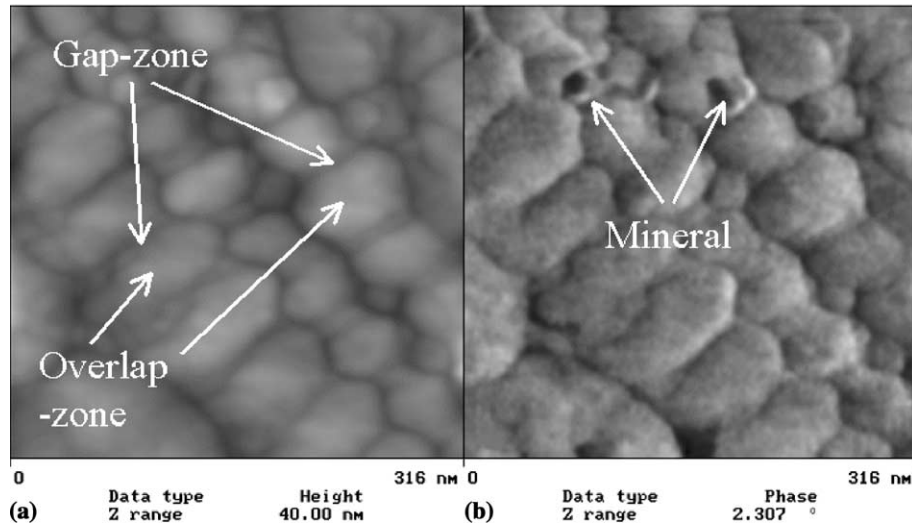


Fig. 4. AFM images of dentin collagen fibrils obtained in liquid. (a) Tapping mode image: gap and overlap zones of adjacent fibrils interlock; (b) phase mode image reveals the presence of mineral particles attached to fibrils.

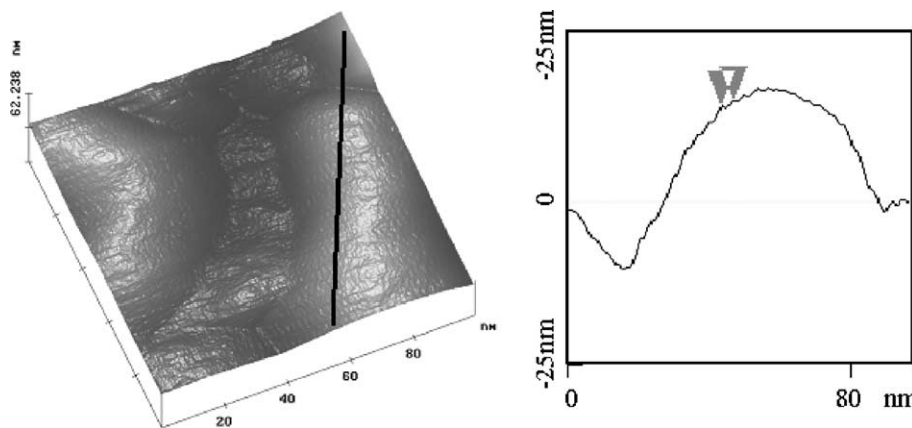


Fig. 5. Tapping mode AFM image obtained in liquid of individual gap zone of collagen fibril and adjacent overlap zones. Section analysis across the diameter of fibril overlap zone reveals subfibrillar structure. Bumps at about 4 nm in distance are associated with microfibrils, the building blocks of collagen type I.

collagen fibrils, which indicate areas of different elastic properties of the substrate. Fig. 5 shows, in a  $100 \times 100$ -nm scanning image, an individual gap zone between two overlap zones of a hydrated collagen fibril. The section profile across the diameter of an overlap zone revealed a subfibrillar structure. Irregular patterns of bumps 2 nm in height appeared at distances of 3.0–4.5 nm from each other. Subfibrillar features of similar sizes also were observed after dehydration. However, they were not present on all fibrils regardless of their state of hydration.

Images with scan sizes below  $1.0 \times 1.0 \mu\text{m}$  were used for section analysis to determine step height and fibril diameter, applying the deconvolution method described above. The axial repeat distance was obtained by Fourier analysis (Fig. 6). The step height between the gap and the overlap zones varied between 3 and 7 nm. Fig. 7a shows the distribution of dentin collagen fibril diameters. Analysis of hydrated collagen revealed three groups of fibril diameters with narrow normal distributions at 83, 91, and 100 nm. Dehydrated collagen fibrils showed a broad distribution of axial diameters between 80 and 105 nm. Fig. 7b shows measurements of the axial repeat distance of collagen fibrils. Axial repeat distances of hydrated collagen fibrils appeared in the range of 54–75 nm, but were predominantly observed within a narrow distribution at 67–68 nm. Drying of the specimens in air resulted in a division of the collagen fibrils into three groups, with axial repeat distances distributed around 57, 62, and 67 nm. The correlation coefficients for axial repeat distances and diameters of hydrated and dehydrated fibrils were 0.17 and  $-0.7$ , respectively, showing that the data for the hydrated fibril are not correlated, while dehydration affects fibril diameter and repeat distance in a reciprocal way. The fibril diameter increases with decreasing axial repeat distance.

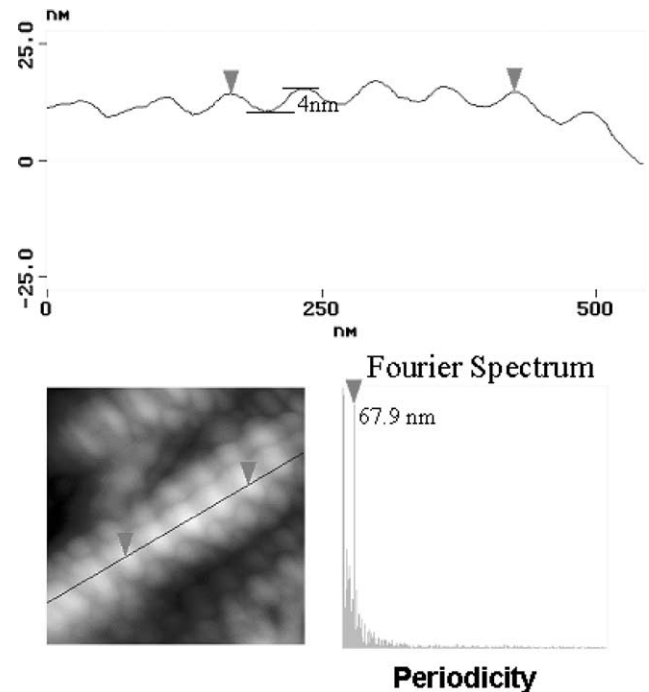


Fig. 6. Section analysis along the axis of a dehydrated fibril shows wave-like repeat pattern. The periodicity of the gap and the overlap zone (D-distance) was determined by Fourier analysis at 67.9 nm. The step height between the gap and the overlap zone was about 4 nm.

#### 4. Discussion

In this study, a chemical process was used to expose type I collagen fibrils of midcoronal dentin. Polished dentin sections prepared from documented human third molars were partially demineralized by citric acid. Acid etching is a common procedure to dissolve the calcium-phosphate mineral phases in dentin in order to form a porous collagenous surface layer, which allows the penetration of a monomer that forms a layer of collagen

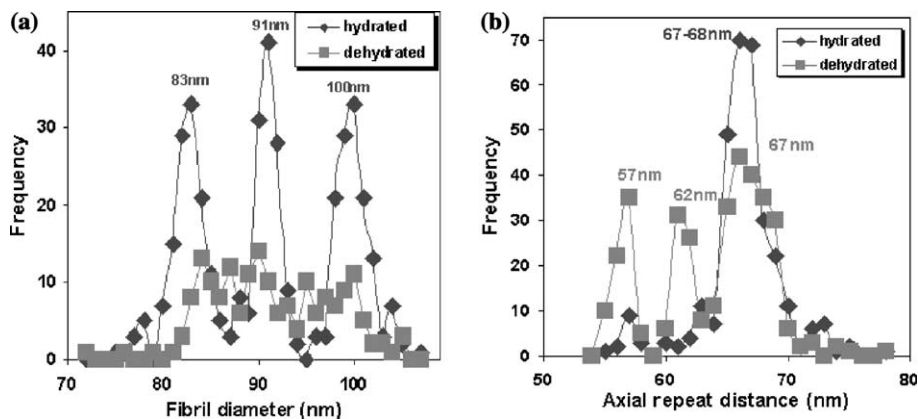


Fig. 7. (a) Plot of the frequency distribution of fibril diameters: three distinguished sizes are observed (83, 91, and 100 nm) for the hydrated fibrils, while dehydration caused a broad distribution between 80 and 105 nm; (b) Distribution of the axial repeat distances: hydrated fibrils show a narrow distribution around 67–68 nm, while dehydration induced grouping of fibril repeat distances at 57, 62, and 67 nm.

and polymer, resulting in a superior interface for the bonding of dental restorations. As shown by several authors (Kinney et al., 1996; Marshall et al., 1997), acid etching produces three zones consisting of a collagen-rich layer superficial to a zone containing a gradient of mineral concentration, which covers the undemineralized dentin substrate. After partial demineralization, samples were immersed into 6.5 vol% NaOCl<sub>aq</sub>, which gradually removed proteins of the extracellular matrix in the collagen-rich zone. At time intervals between 110 and 200 s, the fibrous network of collagen was revealed in situ using AFM. The organization of the collagen framework and the structure of individual collagen fibrils were analyzed. Images at lower resolution showed a random distribution of fibril orientation within the plane imaged (Fig. 2). The fibril axial repeat pattern did not disappear after dehydration (Fig. 3), which is contrary to observations made by El Feninat et al. (2001). The reported layered arrangement of the fibrous network with layers oriented perpendicular to the tubule axes could not be shown due to the limitation of two-dimensional imaging (Kramer, 1951; Wang and Weiner, 1998). However, we frequently observed at higher resolutions (scan sizes below  $1.5 \times 1.5 \mu\text{m}$ ) that adjacent fibrils were interlocked. When fibrils lie parallel to each other, as in Fig. 4, the gap zones come in contact with the overlap zones of adjacent fibrils and thus interlock with each other. It is not certain if this interlocking of fibrils is native to the undemineralized dentin, since after demineralization fibrils are less constrained and might be likely to rearrange into such a configuration. However, it shows that dentin collagen fibrils have the ability to interlock, which is different from observations in tendons, in which fibrils are aligned parallel in a way that gap zones are in contact with the gap zones and overlap zones with the overlap zones of the adjacent fibrils (Arsenault, 1989; Baer et al., 1988; Landis et al., 1991).

Phase mode images at high resolution (Fig. 4b) showed features of about 20 nm located at the transition between the gap and the overlap zone of collagen fibrils. Phase mode becomes sensitive to differences in the elastic response of the tip to the substrate when the set-point amplitude is moderate, but an influence from adhesive interactions and topography cannot be avoided completely (Behrend et al., 1999). The contrast of these particles on collagen is stronger in phase mode than the contrast shown in the topographic mode (Fig. 3a). To obtain such strong contrast as that shown in Fig. 4b, the particles must differ substantially in their elasticity from the underlying organic substrate. We therefore assume that these features represent residual mineral particles on collagen fibrils, which confirms that the acid etching procedure only partially demineralized the substrate. These particles preferentially appeared in the transition from the gap to the overlap zone, which might be related to the location of particular noncollagenous proteins,

e.g., phosphophoryn, that reportedly induce mineralization in collagenous tissues (Begue-Kirn et al., 1998; Dahl et al., 1998; MacDougall et al., 1992; Saito et al., 2000).

Subfibrillar structures could be revealed in air and in liquid only at scan sizes below  $300 \times 300 \text{ nm}$ . Bumps of about 4 nm in width were detected on the surface of cross-sections through the fibril diameter (Fig. 5). In agreement with observations by Baselt et al. (2001), we attribute these nano-features to the presence of microfibrils. In contrast to Baselt et al. (2001), who found subfibrillar structures only if fibrils had been dehydrated, we observed these features also on hydrated fibrils, where they appeared even more pronounced than on dehydrated specimens. Due to the relatively high roughness of etched and bleached dentin surfaces, imaging of these nano-features is difficult and their resolution might predominantly depend on the quality (sharpness and aspect ratio) of the tip, but not necessarily on structural changes induced by hydration. The possibility that these 4-nm bumps are artifactual in origin cannot be ruled out completely at this time. However, the consistency of the size of these bumps at different scan sizes suggests that they are more likely real features associated with the fibril substructure.

New data on the effect of hydration on the fibril structure have been obtained. Analyses of tapping mode AFM images exhibited significant differences in the distribution of fibril diameter and axial repeat distance, depending on the state of hydration of the substrate. Hydrated and dehydrated collagen fibrils varied in their fibril diameters between 75 and 105 nm. While the dehydrated fibrils showed a broad distribution between these values, hydrated fibrils showed a grouping at particular diameters. As shown in Fig. 7a, narrow distributions occurred at diameters of 83, 91, or 100 nm when fibrils were hydrated. According to Holmes et al. (2001), a fibril cross-section of each of these groups would contain approximately 3200, 3550, or 3900 collagen molecules, respectively. Precise measurements of the collagen fibril diameter in dentin are difficult to obtain by electron microscopy, since the random orientation of the fibril makes observations of cross-sections perpendicular to the fibril's axis difficult. This might be a reason for the wide range of diameters (30–120 nm) reported in the literature (Avery, 1988; Lin et al., 1993). In this study we could confirm measurements of dentin collagen made by electron microscopy from several authors (Garberoglio and Brännström, 1976; Pashley, 1991; Perdigao et al., 1996) who observed diameters between 50 and 100 nm for dehydrated fibrils. In contrast, hydrated fibrils showed the unique occurrence of distribution in groups. In the literature, collagen fibril growth has been reported to occur in increments of approximately 8 nm, which was attributed to units of microfibrils added during fibrillogenesis (Prockop and Fertala, 1998). Our findings showed that the mean diam-

eters of the groups differed by 8 or 9 nm, supporting the theory of microfibrils as structural building blocks of collagen fibrils.

Data for distribution functions of the fibril repeat distance were obtained in liquid and dry environments (Fig. 7b). The repeat distance of hydrated fibrils predominantly occurred between 67 and 68 nm, in good agreement with values observed by other authors (Baselt et al., 1993; Chernoff and Chernoff, 1992). It also supports the use of type I collagen specimens as standards for equipment calibration (Wess and Orgel, 2000). After dehydration, the periodicity shortened for some fibrils and showed an overall wider distribution. Besides the 67-nm repeat, two further groups of fibrils with periodicities around 62 and 57 nm occurred. According to XRD and NMR studies (Bella et al., 1995; Price et al., 1997), hydrated fibrils have a higher degree of structural organization or crystallinity. In accordance, our findings of a well-defined axial repeat distance at 67–68 nm and a distribution of the diameter in three defined groups support the observation of an increased structural order in the hydrated fibril. In contrast, dehydration induces structural disorder and mechanical stresses. Adsorbed and chemically bound water evaporates, which destabilizes the quarternary structure of collagen molecules and lowers the degree of organization in the fibril (Bella et al., 1995; Price et al., 1997; Wess and Orgel, 2000). It is assumed that the decreased structural order in the dehydrated fibril causes the fibril diameter to spread over a wide range, between 75 and 105 nm. However, a certain structural arrangement must exist, since the axial repeat pattern remained and showed a distribution in three groups. Furthermore, the effect of partial demineralization and the effect of fibril dissolution from NaOCl on the fibril diameter has to be taken into consideration. Acid etching dissolves the mineral phase gradually. It is assumed that the extrafibrillar mineral is dissolved first, while the intrafibrillar mineral is protected by the collagen molecules and dissolves more slowly. Hence, it is likely that after etching, intrafibrillar mineral is inhomogeneously distributed, which could cause the sometimes irregular appearance of the fibril segments. A test for correlation showed that a decreased axial periodicity of the fibril is associated with an increased fibril diameter. Hence, it is assumed that shrinking of the fibril's long axis is compensated for by a widening of its diameter. However, we did not observe the fibril diameter to increase significantly above 100 nm. Eventually fibrils that still contain most of their intrafibrillar mineral are less affected by dehydration. In contrast, fibrils that are completely demineralized might be altered greatly by dehydration, since the structural support by the mineral is missing. It is assumed that these fibrils are more prone to contract in their longer axis and to bulge out in their diameter as a result of dehydration.

NaOCl attacks proteins nonspecifically and collagen fibrils dissolve during the bleaching process. Hence the fibril diameter can be altered by this treatment. In order to minimize these effects we are currently developing a technique to avoid major alterations of the native fibrillar structure of dentin collagen. This method will include EDTA treatments to dissolve the mineral phase without altering dentin proteins and the use of specific enzymes to digest particular noncollagenous proteins in dentin.

## 5. Conclusions

Etching and controlled deproteinization enabled the *in situ* imaging of the fibrous network of partially demineralized dentin collagen by AFM. Fully hydrated and dehydrated type I collagen fibrils were analyzed at high resolution and information on the organization of the fibrillar network of collagen was obtained. Dehydration induced significant structural changes to the fibrils. While three major groups of fibril diameters were observed when the substrate was hydrated, fibril diameter spread with a broad distribution between 75 and 105 nm after drying. A narrow distribution of the axial repeat distance between 67 and 68 nm was present in hydrated fibrils. Dehydration caused splitting into three groups of axial periodicities at 57, 62, and 67 nm. This new method provides additional insight into the structure and organization of dentin collagen and may contribute to a better understanding of alterations in collagens induced by chemical or biochemical treatments, age, or diseases. Modeling of the fibril structure using this data is encouraged to better understand the effect of dehydration on the molecular level.

## Acknowledgments

AFM-images of Figs. 1c and d are courtesy of Dr. Nil Yücel, Department of Preventive and Restorative Dental Sciences, University of California, San Francisco. This research was supported by NIH/NIDCR, Grant PO1 DE09859.

## References

- Arsenault, A.L., 1989. A comparative electron microscopic study of apatite crystals in collagen fibrils of rat bone, dentin and calcified turkey leg tendons. *Bone Miner.* 6, 165–177.
- Avery, J.K., 1988. *Oral Development and Histology*. B.C. Dekker Inc., Toronto, Philadelphia.
- Baer, E., Cassidy, J.J., Hiltner, A., 1988. Hierarchical structure of collagen and its relationship to the physical properties of tendon. In: Nimni, M.E. (Ed.), *Collagen: vol. II, Biochemistry and Biomechanics*. CRC Press, Boca Raton, FL, p. 5v.

- Baselt, D.R., Revel, J.P., Baldeschwieler, J.D., 1993. Subfibrillar structure of type I collagen observed by atomic force microscopy. *Biophys. J.* 65, 2644–2655.
- Begue-Kirn, C., Krebsbach, P.H., Bartlett, J.D., Butler, W.T., 1998. Dentin sialoprotein, dentin phosphoprotein, enamelysin and ameloblastin: tooth-specific molecules that are distinctively expressed during murine dental differentiation. *Eur. J. Oral Sci.* 106, 963–970.
- Behrend, O.P., Odoni, L., Loubet, J.L., Burnham, N.A., 1999. Phase imaging: deep or superficial? *Appl. Phys. Lett.* 75, 2551–2553.
- Bella, J., Brodsky, B., Berman, H.M., 1995. Hydration structure of a collagen peptide. *Structure* 3, 893–906.
- Brodsky, B., Tanaka, S., Eikenberry, E.F., 1988. X-ray diffraction as a tool for studying collagen structure. In: Nimni, M.E. (Ed.), *Collagen: vol. I, Biochemistry*. CRC Press, Boca Raton, FL, p. 5v.
- Burnham, N.A., Behrend, O.P., Oulevey, F., Gremaudi, G., Gallo, P.J., Gourdon, D., Dupas, E., Kulik, A.J., Pollock, H.M., Briggs, G.A.D., 1997. How does a tip tap? *Nanotechnology* 8, 67–75.
- Chen, C.H., Hansma, H.G., 2000. Basement membrane macromolecules: insights from atomic force microscopy. *J. Struct. Biol.* 131, 44–55.
- Chernoff, E.A.G., Chernoff, D.A., 1992. Atomic force microscope images of collagen fibers. *J. Vac. Sci. Technol. A* 10, 596–599.
- Dahl, T., Sabsay, B., Veis, A., 1998. Type I collagen–phosphoryn interactions: specificity of the monomer–monomer binding. *J. Struct. Biol.* 123, 162–168.
- Di Renzo, M., Ellis, T.H., Sacher, E., Stangel, I., 2001. A photoacoustic FTIRS study of the chemical modifications of human dentin surfaces: II. Deproteinization. *Biomaterials* 22, 793–797.
- El Feninat, F., Ellis, T.H., Sacher, E., Stangel, I., 2001. A tapping mode AFM study of collapse and denaturation in dentinal collagen. *Dent. Mater.* 17, 284–288.
- Garberoglio, R., Brännström, M., 1976. Scanning electron microscopic investigation of human dentinal tubules. *Arch. Oral Biol.* 21, 355–362.
- Goldberg, M., Takagi, M., 1993. Dentine proteoglycans: composition, ultrastructure and functions. *Histochem. J.* 25, 781–806.
- Hansma, H.G., 2001. Surface biology of DNA by atomic force microscopy. *Annu. Rev. Phys. Chem.* 52, 71–92.
- Holmes, D.F., Graham, H.K., Trotter, J.A., Kadler, K.E., 2001. STEM/TEM studies of collagen fibril assembly. *Micron* 32, 273–285.
- Kinney, J.H., Haupt, D.L., Balooch, M., White, J.M., Bell, W.L., Marshall, S.J., Marshall Jr., G.W., 1996. The threshold effects of Nd and Ho: YAG laser-induced surface modification on demineralization of dentin surfaces. *J. Dent. Res.* 75, 1388–1395.
- Kinney, J.H., Pople, J.A., Marshall, G.W., Marshall, S.J., 2001. Collagen orientation and crystallite size in human dentin: a small angle X-ray scattering study. *Calcif. Tissue Int.* 69, 31–37.
- Kramer, I.R.H., 1951. The distribution of collagen fibrils in the dentin matrix. *Br. Dent. J.* 91, 1–7.
- Landis, W.J., Moradian-Oldak, J., Weiner, S., 1991. Topographic imaging of mineral and collagen in the calcifying turkey tendon. *Connect. Tissue Res.* 25, 181–196.
- Lee, R.M.K.W., 1984. A critical appraisal of the effects of fixation, dehydration and embedding on cell volume. In: Revel, J.-P. (Ed.), *The Science of Biological Specimen Preparation for Microscopy and Microanalysis*. AFM Scanning Electron Microscopy, Chicago.
- Lees, S., Capel, M., Hukins, D.W., Mook, H.A., 1997. Effect of sodium chloride solutions on mineralized and unmineralized turkey leg tendon. *Calcif. Tissue Int.* 61, 74–76.
- LeGeros, R.Z., 1991. Calcium phosphates in oral biology and medicine. *Monogr. Oral Sci.* 15, 1–201.
- Lin, C.P., Douglas, W.H., Erlandsen, S.L., 1993. Scanning electron microscopy of type I collagen at the dentin–enamel junction of human teeth. *J. Histochem. Cytochem.* 41, 381–388.
- Linde, A., Robins, S.P., 1988. Quantitative assessment of collagen crosslinks in dissected predentin and dentin. *Coll. Relat. Res.* 8, 443–450.
- MacDougall, M., Zeichner-David, M., Murray, J., Crall, M., Davis, A., Slavkin, H., 1992. Dentin phosphoprotein gene locus is not associated with dentinogenesis imperfecta types II and III. *Am. J. Hum. Genet.* 50, 190–194.
- Marshall, G.W., Yücel, N., Balooch, M., Kinney, J.H., Habelitz, S., Marshall, S.J., 2001. Sodium hypochlorite alterations of dentin and dentin collagen. *Surf. Sci.* 491, 444–455.
- Marshall Jr., G.W., Balooch, M., Tench, R.J., Kinney, J.H., Marshall, S.J., 1993. Atomic force microscopy of acid effects on dentin. *Dent. Mater.* 9, 265–268.
- Marshall Jr., G.W., Marshall, S.J., Kinney, J.H., Balooch, M., 1997. The dentin substrate: structure and properties related to bonding. *J. Dent.* 25, 441–458.
- Nimni, M.E., Harkness, R.D., 1988. Molecular structures and functions of collagens. In: Nimni, M.E. (Ed.), *Collagen: vol. I, Biochemistry*. CRC Press, Boca Raton, FL, pp. 1–79.
- Parry, D.A.D., Craig, A.S., 1988. Collagen fibrils during development. In: Nimni, M.E. (Ed.), *Collagen*. CRC Press, Boca Raton, FL, pp. 1–20.
- Pashley, D.H., 1991. Clinical correlations of dentin structure and function. *J. Prosthet. Dent.* 66, 777–781.
- Perdigão, J., Lambrechts, P., van Meerbeek, B., Tome, A.R., Vanherle, G., Lopes, A.B., 1996. Morphological field emission–SEM study of the effect of six phosphoric acid etching agents on human dentin. *Dent. Mater.* 12, 262–271.
- Perdigão, J., Thompson, J.Y., Toledano, M., Osorio, R., 1999. An ultra-morphological characterization of collagen-depleted etched dentin. *Am. J. Dent.* 12, 250–255.
- Pereira, W.E., Hoyano, Y., Summons, R.E., Bacon, V.A., Duffield, A.M., 1973. Chlorination studies. II. The reaction of aqueous hypochlorous acid with  $\alpha$ -amino acids and dipeptides. *Biophys. Acta* 313, 170–180.
- Price, R.I., Lees, S., Kirschner, D.A., 1997. X-ray diffraction analysis of tendon collagen at ambient and cryogenic temperatures: role of hydration. *Int. J. Biol. Macromol.* 20, 23–33.
- Prockop, D.J., Fertala, A., 1998. The collagen fibril: the almost crystalline structure. *J. Struct. Biol.* 122, 111–118.
- Raspanti, M., Alessandrini, A., Ottani, V., Ruggeri, A., 1997. Direct visualization of collagen-bound proteoglycans by tapping-mode atomic force microscopy. *J. Struct. Biol.* 119, 118–122.
- Reedy, M.C., Reedy, M.K., Goody, R.S., 1983. Co-ordinated electron microscopy and X-ray studies of glycerinated insect flight muscle. II. Electron microscopy and image reconstruction of muscle fibres fixed in rigor, in ATP and in AMPPNP. *J. Muscle Res. Cell Motil.* 4, 55–81.
- Revenko, I., Sommer, F., Minh, D.T., Garrone, R., Franc, J.M., 1994. Atomic force microscopy study of the collagen fibre structure. *Biol. Cell* 80, 67–69.
- Saito, T., Yamauchi, M., Abiko, Y., Matsuda, K., Crenshaw, M.A., 2000. In vitro apatite induction by phosphoryn immobilized on modified collagen fibrils. *J. Bone Miner. Res.* 15, 1615–1619.
- Saito, T., Yamauchi, M., Crenshaw, M.A., 1998. Apatite induction by insoluble dentin collagen. *J. Bone Miner. Res.* 13, 265–270.
- Scheuring, S., Fotiadis, D., Moller, C., Muller, S.A., Engel, A., Muller, D.J., 2001. Single proteins observed by atomic force microscopy. *Single Mol.* 2, 59–67.
- Takeyasu, K., Omote, H., Nettikadan, S., Tokumasu, F., Iwamoto-Kihara, A., Futai, M., 1996. Molecular imaging of *Escherichia coli* F0F1-ATPase in reconstituted membranes using atomic force microscopy. *FEBS Lett.* 392, 110–113.
- Ten Cate, A.R., 1994. *Oral histology: Development, Structure, and Function*, fourth ed. Mosby, St. Louis.

- Wang, R., Weiner, S., 1998. Human root dentin: structural anisotropy and Vickers microhardness isotropy. *Connect. Tissue Res.* 39, 269–279.
- Wassen, M.H., Lammens, J., Tekoppele, J.M., Sackers, R.J., Liu, Z., Verbout, A.J., Bank, R.A., 2000. Collagen structure regulates fibril mineralization in osteogenesis as revealed by cross-link patterns in calcifying callus. *J. Bone Miner. Res.* 15, 1776–1785.
- Weiner, S., Wagner, H.D., 1998. The material bone: structure–mechanical function relations. *Annu. Rev. Mater. Sci.* 28, 271–298.
- Wess, T.J., Orgel, J.P., 2000. Changes in collagen structure: drying, dehydrothermal treatment and relation to long term deterioration. *Thermochim. Acta* 365, 119–128.
- White, J.M., Goodis, H.E., Marshall, S.J., Marshall, G.W., 1994. Sterilization of teeth by gamma radiation. *J. Dent. Res.* 73, 1560–1567.